

Study of intraseasonal variability of Indian summer monsoon using a regional climate model

P. Maharana¹ · A. P. Dimri¹

Received: 28 August 2014 / Accepted: 24 April 2015 / Published online: 7 May 2015
© Springer-Verlag Berlin Heidelberg 2015

Abstract The Indian summer monsoon season is very heterogeneous over Indian land mass from precipitation point of view. The intraseasonal variability of the rainfall during summer is marked by the active and break spells of the rainfall. The regional climate model version 4.0 (RegCM4.0) forced with European centre of medium range weather forecast interim reanalysis (ERA-Int) is used to examine the intraseasonal variability and meteorological processes associated with it. The model rightly represents the climatology of different fields such as the surface temperature, sea level pressure, lower level wind and the precipitation for monsoon season. The model captures the different active and break spells and the results are in agreement with the observed value and previous studies. The major features of the active/break periods, such as the positive/negative rainfall anomaly over the monsoon core region (MCR) and negative/positive rainfall anomaly over the foothills of Himalayas and southern part of India is nicely represented in the model. The model rightly reproduces the evolution of the active and break phase and also the revival from the break period by the northward propagation of active rainfall anomaly. The heat trough type of circulation is analysed in detail along with the atmospheric condition during active and break spell over the MCR. The atmospheric condition over MCR resembles the heat trough type circulation during break spells. The moisture availability, moisture–precipitation relation and their transition during active and break period over the MCR is established.

Keywords Intraseasonal variability · Regional climate model · Active and break spells · Monsoon core region

1 Introduction

Indian region gets monsoonal rainfall during summer (June–September: JJAS hereafter) because of the southwest monsoon. Indian summer monsoon (ISM) contributes 80 % of the total annual rainfall over India. Within summer, the rainfall during July and August (JA hereafter) are more as compare to the other 2 months and hence these 2 months contribute maximum to the total summer monsoonal rainfall. The rainfall pattern during ISM shows wide range of temporal as well as spatial variability over the Indian region, such as one part of the country flooded and at the same time other part having drought like conditions. The rainfall also varies at a daily, sub-seasonal, interannual or decadal time scale during ISM. This intraseasonal variability phenomenon is widely studied by various researchers using various observational data sets such as the station data, satellite data and the gridded rainfall data from various available sources (Goswami et al. 1998, 2006a, b; Hoyos and Webster 2007; Kripalani et al. 2004; Krishnamurthy and Shukla 2000; Kulkarni et al. 2006; Rajeevan et al. 2006, 2010; Rajeevan and Bhatte 2008). The rainfall during monsoon months is not uniform and there are times when excess/deficit rainfall occurs and thus termed as the active/break phases of ISM. The synoptic disturbances originate over the Indian Ocean and its surrounding regions have a large influence on the ISM rainfall which leads to active and break spells during its course. The intraseasonal variability of the rainfall during ISM also exhibits in the form of different days of oscillations. The major modes of the oscillations are 3–6 days, 1–20 days, 30–60 days and

✉ A. P. Dimri
apdimri@hotmail.com

¹ School of Environmental Sciences, Jawaharlal Nehru University, New Delhi 110067, India

122 days (Mohapatra and Mohanty 2007). The long intense spell of active and break spell have a greater impact on the seasonal rain (Gadgil and Joseph 2003). The long intense active (break) spell can lead to excess rainfall (drought) situation during ISM. During normal years, the long active (break) spell may cause flood (drought) like condition. This active and break periods have very critical role on the Indian agriculture and thus can influence the yield. Since the intraseasonal variability of the rainfall play a major role in the field of Indian agriculture, economy and water resource management, hence the prediction of the active and break spells of ISM, their duration, and intensity is really important. It is thus important to analyze the synoptic atmospheric process involved during the active and break spells.

The study of the intraseasonal variability or the active and break spells of the ISM has been widely studied using the station data (Raghavan 1973; Kripalani et al. 2004; Mohapatra and Mohanty 2007), reanalysis datasets (Goswami et al. 1998; Krishnan et al. 2000; Goswami and Ajaya Mohan 2001; Vecchi and Harrison 2002; Klingaman et al. 2008; Misra et al. 2012), different gridded observations (Krishnamurthy and Shukla 2000; Hartmann and Michelsen 1989; Krishnamurthy and Shukla 2007; Rajeevan et al. 2006; Panchawagh and Vaidya 2011; Halder et al. 2012) and different observational datasets (Chen and Chen 1993; Goswami et al. 2006b). In addition, several modelling studies have been carried out to understand the intraseasonal processes associated with the ISM. The ability of the climate models to capture the seasonal precipitation anomalies depends upon the ability of the climate model to capture the climatological distribution of the summer rainfall and the intraseasonal variability. So the ability of the model to simulate the regional features of the summer monsoon precipitation and the climatology of the intraseasonal oscillations (ISOs) with an acceptable degree of fidelity is essential for it to be used for prediction of seasonal mean (Ajayamohan 2007). The intraseasonal variability have been studied using Atmospheric global circulation models (AGCMs) by various researchers such as Goswami et al. 1998; Fu et al. 2002; Goswami and Xavier 2005; Abhik et al. 2013; Ajayamohan 2007). Although recently the efficiency and efficacy of the models have increased but still they have not shown improvement over the ISM zone (Kang et al. 2002). Several researchers used coupled climate model to study the intraseasonal variability of ISM (Lal et al. 2000; Achuthavarier and Krishnamurthy 2009; Ajayamohan and Goswami 2007; Goswami et al. 2012). The skill of the regional climate models (RCMs) also experimented by many scientist to study the intraseasonal variability (Bhaskaran et al. 1998; Bhate et al. 2012; Taraphdar et al. 2010; Samala et al. 2013).

Apart from the active and break day, various researches also study the intraseasonal variation of rainfall exhibited in the form of different days of oscillation within the ISM (Chen and Chen 1993; Hartmann and Michelsen 1989; Klingaman et al. 2008). They try to establish several reasons for the intraseasonal variation of the ISM. Krishnan et al. (2000) showed the initiation of the breaks spell is marked by the abrupt movement of anomalous Rossby wave from Bay of Bengal (BoB) into north-west and central India. Vecchi and Harrison (2002), using satellite data, showed that the sub-seasonal cooling of SST over BOB precedes the monsoon break by 1 week and it is very useful for prediction of short term monsoon variability. Goswami et al. (2006b) found that the limited predictability of the Asian summer monsoon appears to be due to the fact that the contribution from external interannual variability (the interannual variability contributed by the factors such as the air-sea interaction, local heating, land-surface processes etc.) over the region is relatively weak and comparable to that from internal interannual variability (the interannual variability contributed by the internal model processes and physics options chosen during model simulation). Mohapatra and Mohanty (2007) show the synoptic scale monsoon disturbance or low pressure systems originated over the north BOB and their subsequent movement towards the monsoon trough and persistence is the main reason of intraseasonal variability over Odisha. Halder et al. (2012) used Tropical Rainfall measuring Mission (TRMM) data to analyse the role of clouds hydrometeors in the northward propagation of the monsoon intra seasonal oscillation. He established that during northward propagation the cloud water leads and the cloud ice lags. Krishnamurthy and Shukla (2000) reported that, during the major drought years, the large scale negative anomalies of rainfall covers the Indian region for most of the monsoon season and also the nature of the intra seasonal variability like the active and break phase are is not different during excess and deficit monsoon years.

The study related to the intraseasonal variability of monsoon is very important as a major chunk of the population of India depends upon the agricultural activity. The better understanding of intraseasonal variability may help them to plan their cropping, which ultimately related to their socio-economic upliftment. Although several earlier studies has been done to understand the intraseasonal variability of the ISM, but still the study of the intraseasonal variability of ISM and the propagation of the active and break spell over the Indian region using a RCM is very limited. The objective of this work is to analyse the intraseasonal variability and the propagation characteristics of the ISM over the monsoon core region (MCR) using a RCM (RegCM4.0) forced with a improved initial and boundary conditions from ERA-Int (Dee et al. 2011) The MCR is a region where the largest fluctuation of rainfall anomaly occurs

during the active and break spells. The robustness of the model depends on its capacity to capture the intraseasonal variability as well as the atmospheric processes associated with it. The study also concerns the ability of the model to capture the evolution and progress of the active and break spells the heat trough type circulation and the moisture-precipitation relation during the active and break phases over the MCR.

In this study, Sect. 2 explains the model details, experimental design and the description of the datasets used in this study. Section 3 deals with the climatological analysis of the different meteorological fields to check the ability of the RCM to simulate the ISM. In Sect. 4, the details of the criterion for choosing the MCR and the criterion for defining the active and break spell are discussed in detail. The comparison of the simulated active and break spell with the earlier studies are made in the Sect. 5. The Sect. 6 deals with the evolution of the active and break phase and the meteorological representation of different fields over the Indian region. The major features of the intense long break, heat trough type meridional circulation (Rajeevan et al. 2010) and the modelling analysis of this process is described in Sect. 7. Section 8 includes the discussion and the concluding remarks of this study.

2 Model details, data used and experimental design

A regional climate model named RegCM4.0 (Giorgi et al. 2012) forced with ERA-Interim reanalysis is used to carry out the necessary simulation from 1989 to 2005. This period is chosen as corresponding IMD observations (at $0.5^\circ \times 0.5^\circ$) are initially available for the period 1971–2005 (Rajeevan and Bhat 2008). The RegCM was first developed at NCAR and the further development is made at International Centre for Theoretical Physics (ICTP), Trieste, Italy. RegCM4.0 is an upgraded version of RegCM3 (Pal et al. 2007; Giorgi et al. 2012). RegCM4.0 has similar hydrostatic version of the dynamical core of MM5 (Grell et al. 1994). The NCAR CCM3 scheme (Kiehl et al. 1996) is used by the model for the radiation parameterization. The Biosphere–Atmosphere Transfer Scheme (Dickinson et al. 1993) and its surface physics included which incorporates the role of vegetation and exchange of water vapour, momentum and energy between land surface and atmosphere. It includes the surface scheme over the ocean (Zeng et al. 1997) and planetary boundary scheme developed by Holtlag and Boville (1993). Grell convective precipitation scheme (Grell 1991) is used with Fritsch and Chappell closure assumptions (Fritsch and Chappell 1980). The selection of the convective precipitation scheme is based on the sensitivity test done prior to the simulation. The elevation and the land use

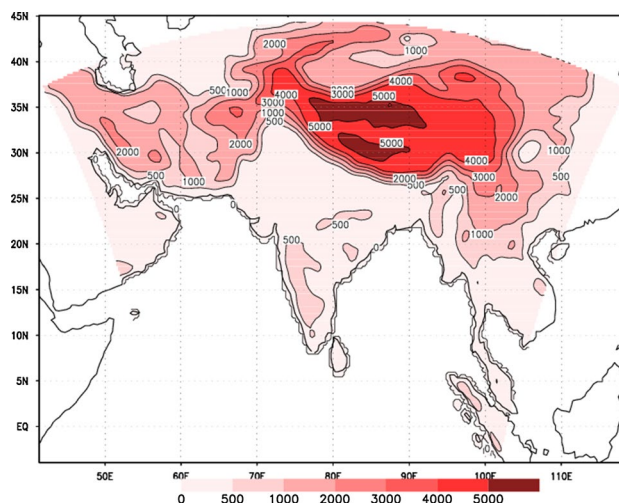


Fig. 1 Model simulated domain showing the topography (m; shaded)

and vegetation are taken from United States Geological Survey and Global Land Cover Characterization respectively. Terrain heights and land use data at 30 min resolution are downloaded from <http://users.ictp.it/~pubregcm/RegCM4/globedat.htm#part4>. The model simulation are very sensitive to the selection of the domain, so the domain is chosen carefully in such a way that the domain selected for the simulation is sufficiently large to produce its own large scale circulation and small grid scale features (Jones et al. 1995). Also the region over which the analysis has been carried out is sufficiently away from the boundary to avoid unrealistic responses to the internal forcing (Seth and Giorgi 1998; Maharana and Dimri 2014a). The model domain selected for the simulation is shown in Fig. 1.

17 years of model simulation (1989–2005) is made using RegCM4.0 to study the model performance, its ability to capture the intraseasonal variability and associated processes over the Indian region. The ERA-Interim at a horizontal resolution of $1.5^\circ \times 1.5^\circ$ with 37 pressure levels is used as the initial and boundary condition, updating at every 6 h, to run the model simulation. The SST forcing used for the simulation is Optimum Interpolation Sea Surface Temperature (OISST) taken from the National Oceanic and Atmospheric Administration (NOAA) at a resolution of $1^\circ \times 1^\circ$ (Reynolds et al. 2002). The simulations in this study over the Indian domain (Fig. 1) are made at a horizontal resolution of 50 km. The horizontal resolution chosen in the study is fine enough to study the meso-scale processes like the ISM. The centre point of the model domain is 80°E and 20°N . The east–west extent of the model is up to 120 grid points and the north–south extent is up to 101 grid points. The number of vertical layers chosen is 18. The model is integrated at 180 s time step. The domain is chosen in such a way that its spatial extent included the BoB, Arabian Sea

Table 1 Model details

Model	RegCM4.0
Dynamics	MM5 hydrostatic (Grell et al. 1994)
Main prognostic variables	u, v, t, px, ts
Map projection	Lambert conformal map projection
Central point of domain	Longitude: 80°N latitude: 20°E
Number of horizontal grid points	120,101 grid points for x, y respectively
Horizontal grid distance	50 km
Number of vertical levels	18 σ levels
Horizontal grid scheme	Arakawa-Lamb B grid staggering
Time integration scheme	Split explicit
Lateral boundary conditions	ERAIN (1989–2008)
Radiation scheme	CCM3
Planetary boundary layer Parameterization schemes	Non-local, counter-gradient (Holtslag and Boville 1993)
Convective precipitation scheme	Grell (Grell et al. 1994), Frisch and Chappell closure assumptions
Soil model	High resolution soil model
Topography	USGS
Surface parameters	BATS1E (Dickinson et al. 1993)
SST	OIWK

and the Indian landmass along with the Himalayas. The model details are given in Table 1.

The RegCM4.0 model simulated precipitation is compared over the Indian land points with the India Meteorological Department (IMD) gridded precipitation ($0.5^\circ \times 0.5^\circ$) (Rajeevan and Bhat 2008). The model circulation is validated with ERA-In daily wind (Dee et al. 2011) which is available at a grid spacing of $1.5^\circ \times 1.5^\circ$.

3 Climatology of different meteorological field

During summer, the higher temperature over the land heats up the surface air. This warm air being lighter rises up and thus creates low pressure over the Indian landmass as compare to seas. This pressure gradient drives the moisture laden air from the sea towards the Indian land mass. The moisture laden air on interaction with the Indian orography causes precipitation over land. Figure 2a–c shows the JJAS climatology (1989–2005) of the surface air temperature of model, CRU observation and their respective bias. The model simulated spatial distribution of the temperature over India shows the heat low ($30\text{--}35^\circ\text{C}$) over north-western part of India and the temperature ranging from 25 to 30°C over rest of the Indian land mass. The land-sea temperature contrast during summer is nicely reproduced by the model. The bias plot (Fig. 2c) depicts that the model performs very well over the central and north-west part of India with less cold bias, but the southern and northern part of the country shows cold bias of $2\text{--}4^\circ\text{C}$. The cold bias in the model attributed to the excess rainfall and its evaporation, which

causes more cooling in the model environment (Fig. 2f). Similar results were reported by Maharana and Dimri (2014b).

Figure 2d–f illustrates the JJAS precipitation climatology of model, IMD observation and their bias respectively. The simulated climatological precipitation is more than 21 mm/day over Western-Ghats, varies from 6 to 9 mm/day over central India and $18\text{--}21$ mm/day over northeast. The corresponding IMD observation shows the precipitation is more than 21 mm/day over Western-Ghats and northeast, and ranges from 3 to 12 mm/day over the central Indian region. The climatological value of JJAS precipitation averaged over India is 87.6 cm which is very close to the corresponding observed value of 82.1 cm for the period 1989–2005. The model nicely able to represent the spatial distribution of rainfall over India, along with the major rainfall peaks such as the western-Ghats and the northeast and also the central Indian part. The bias plot (Fig. 2f) shows a wet bias ranging from 4 to 10 mm/day over Western-Ghats and $2\text{--}4$ mm/day over the Indo-Gangetic plains. But central Indian region shows a dry bias of $2\text{--}6$ mm/day. The central India gets rainfall due to the landfall of the monsoon disturbances, which are originated over the BoB. The Findlater Jet at lower level brings in the moisture over India which in interaction with the Western-Ghats causes heavy orographic precipitation over this region which might not be clearly represented in the gridded observational dataset and hence shows wet bias over this region. The leeward side of the Western-Ghats and the central India get less rainfall due to the lesser availability of the moisture. Also, the higher temperature over the BoB reduce the moisture availability

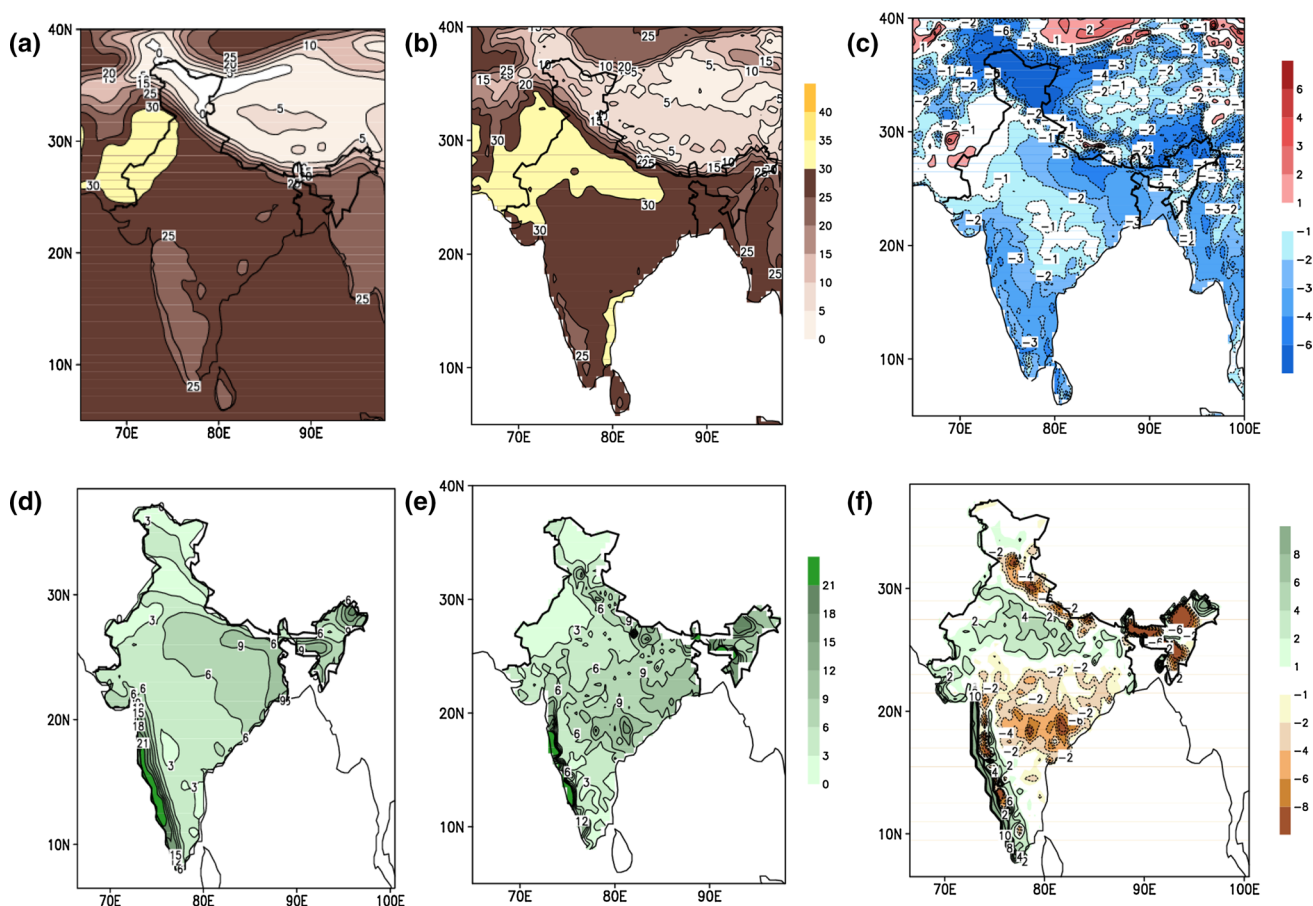


Fig. 2 JJAS average temperature ($^{\circ}\text{C}$; shaded) in **a** model, **b** observation and **c** their respective bias (model-observation). Similarly the *second* row represents the JJAS average precipitation (mm/day) in **d** model, **e** observation and **f** their respective bias

over the sea, so the monsoon disturbances originating over the BoB which falls over the MCR and also BoB branch which is going towards the northeast have less available moisture. Further, the JJAS climatological moisture flux and transport is examined to explain the dry bias over the central India (Figure not shown). The analysis shows that the magnitude of the moisture flux over the BoB is less in the model as compare to the ERA-Int observation and also the model simulated strength of transport over the central India is high as compare to the observed value. This implies that less moisture moves towards the central India and quickly transported away from this region in the model. So the rainfall is less in model as compare to the observation and hence the model shows dry bias over central India. Similar findings using a regional climate model were also reported in the previous studies (Maharana and Dimri 2014b).

The simulated wind at lower (850 hPa) and upper level (200 hPa) is validated against the ERA-Int wind. Figure 3a–c illustrates the climatological simulated lower level wind, the observed value and their bias respectively. The

model able to reproduce the major lower level wind features such as the position of the core of the Findlater jet, its strength over sea (15 m/s) and over land (9–12 m/s). The lower level wind bias plot shows the position; spatial extent and the strength of the Findlater jet are well captured by the model over sea and land (Fig. 3c). The model shows an easterly bias of 2–4 m/s over southern India and westerly bias of the Uttarakhand region. The model wind at finer resolution might able to resolve the interaction of wind and topography and hence give rise to the bias but still the model is good enough to capture the mean low level wind during the monsoon over India.

Figure 3d–f represents the upper level climatological wind (200 hPa) in the simulation, ERA-Int observation and their respective bias. The major features of the upper level wind such as the Tibetan anticyclone, tropical easterly jet and subtropical westerly jet stream and their position are nicely captured by the model. The tropical easterly jet, which covers the southern peninsula have a maximum strength of 20 m/s and the subtropical westerly jet has maximum strength 30 m/s are well reproduce by the model.

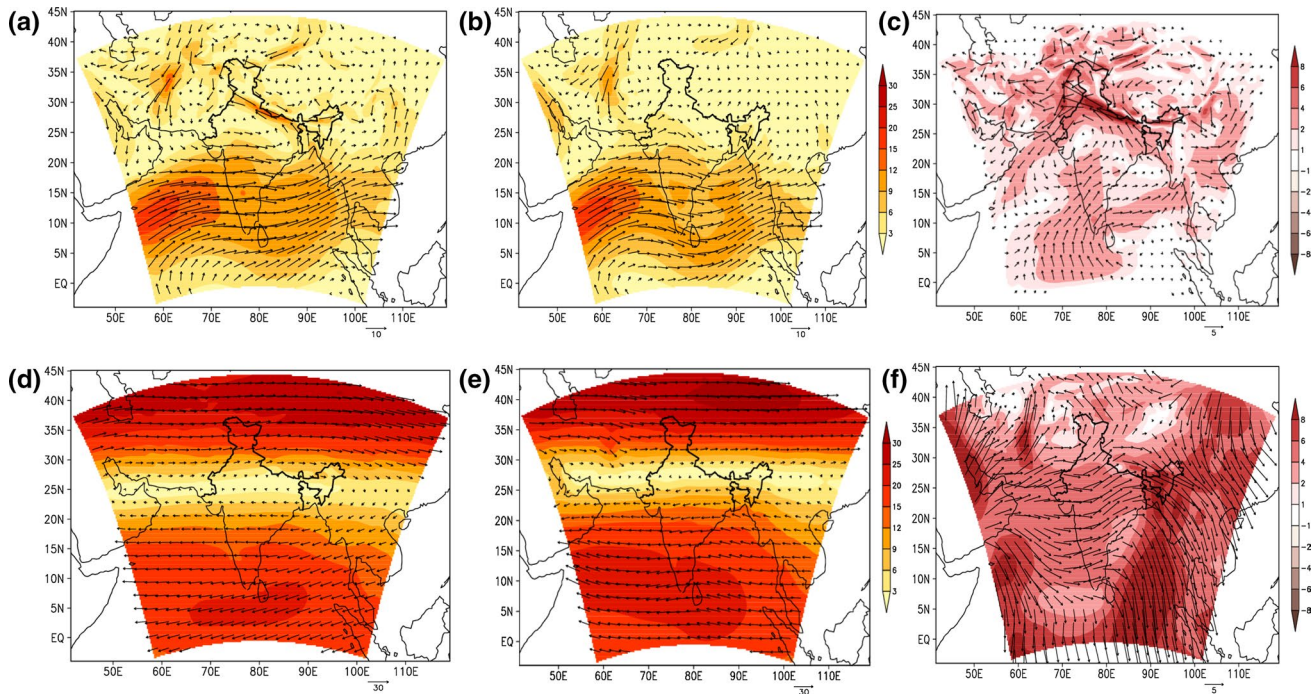


Fig. 3 JJAS average wind (m/s; magnitude is shaded and direction is shown in vector) **a** model, **b** corresponding verification reanalysis and **c** Bias at 850 hPa and **d** model, **e** corresponding verification reanalysis and **f** Bias at 200 hPa respectively

Figure 3f illustrates the JJAS wind bias at upper level. The tropical easterly jet shows a westerly bias of 4–6 m/s where as the subtropical easterly jet has a easterly bias of 1–2 mm/day. The position of the Tibetan anticyclone has slightly shifted southward in the simulation.

The basic climatological features of the ISM are well represented by the model such as the land sea temperature difference, the pressure gradient between the land and sea (figure not shown) and the Findlater jet (at 850 hPa) over the Arabian Sea which carries moisture towards the Indian land and cause precipitation. The major rainfall peaks over India such as the Western Ghats, northeast and the central India are well represented with spatial accuracy. As the synoptic representation of different meteorological parameters and their basic climatological features are captured in the simulation, so the daily model output is taken for the analysis of the intraseasonal variability during ISM.

4 Defining the monsoon core region and the methodology for calculation of active and break spells

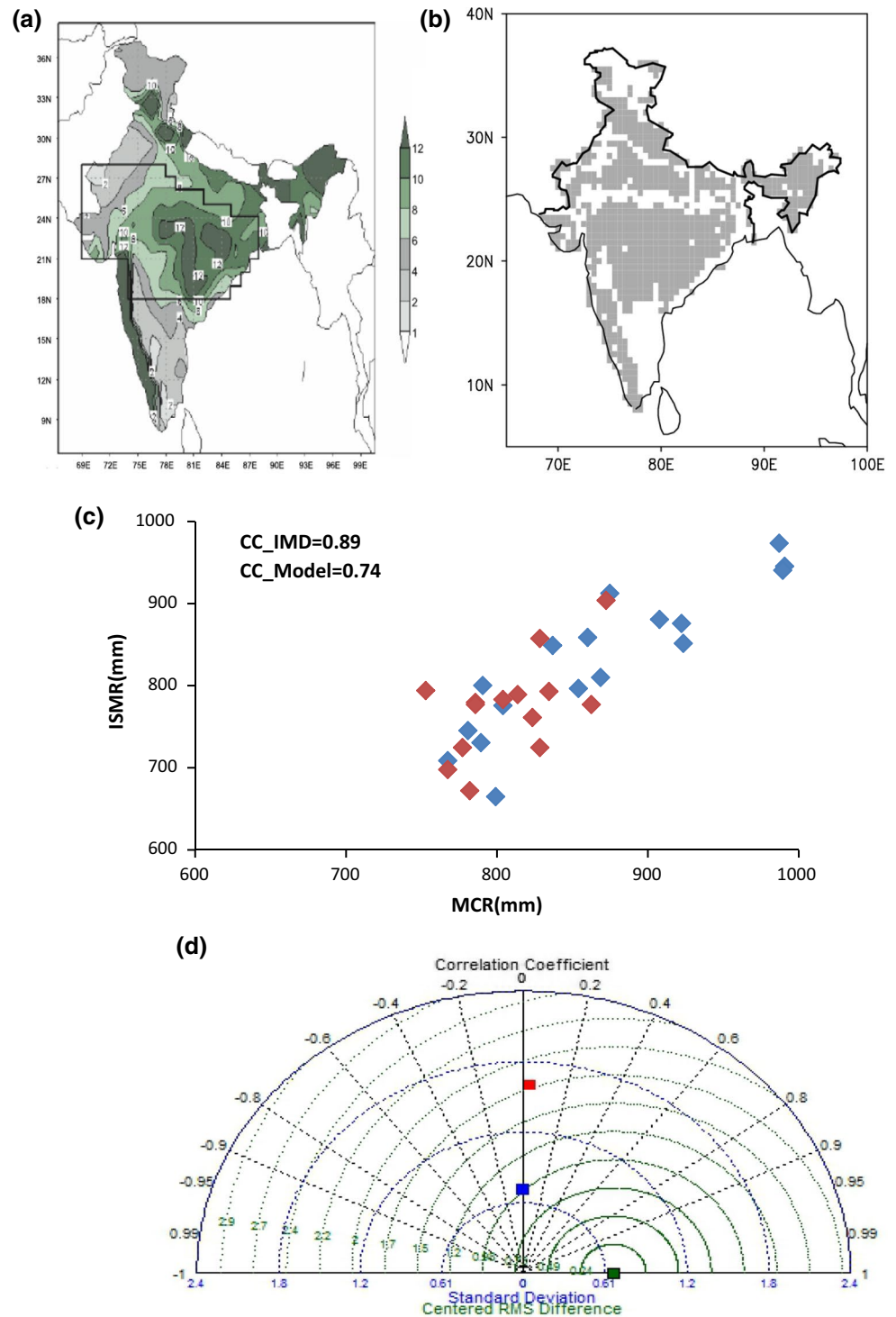
The whole Indian landmass is characterized by the heterogeneous distribution of rainfall during summer. But in most of the earlier studies, the all India rainfall average is used to study the active and break spells. Krishnamurthy and Shukla (2000) analyzed the dominant modes of the daily

rainfall anomaly and reported that the sign of the rainfall anomaly over the central India is opposite to that of the foothills of the Himalayas and that of the southern India. The rainfall over the central India is high during the active spell of the Indian monsoon. During break spells the monsoon trough shifts to the foothills of Himalayas causing an increase in the rainfall over the foothill states of Himalayas and southern Indian (Gadgil and Joseph 2003). These studies conclusively point towards a region over the central India where majority of rainfall occurs during summer monsoon and which can be a representative zone of the total Indian landmass.

Figure 4a shows the MCR taken for the study by Rajeevan et al. (2010) which lies roughly between 18–28°N and 65–88°E. The rainfall over this region and its fluctuation in the monsoon season may be attributed to the establishment of the tropical convergence zone and its movement north and south from its position. The same area has been selected for the present study as chosen by Rajeevan et al. (2010) (Rajeevan study hereafter). They described that utmost care has been taken to define the MCR; careful exclusion of the foot hills region of Himalayas is done where rainfall is very high during the break period.

Initially, few statistical experiments are performed in order to establish a relation whether the rainfall over the chosen area or the MCR for this study is a true representative of whole Indian rainfall. A two tailed student's *t* test is done for the JJAS rainfall of the model and IMD

Fig. 4 **a** The monsoon core zone defined by Rajeevan et al. (2010) and the shaded part shows the magnitude of precipitation. **b** Student's *t* test for JJAS precipitation climatology between RegCM4.0 and IMD, the shaded region shows the area with 95 % significance. **c** Scattered plot and the correlation coefficient between all Indian summer monsoon rainfall and the rainfall in the monsoon core zone (red points are for the model and the blue points for the IMD observation) and **d** Taylor diagram of the model with respect to IMD observational datasets and the ERA-Int reanalysis (red colour solid square represents the IMD observation, blue square represents the ERA-Int reanalysis and green square represents the model)



observation at 95 % confidence level for 1989–2005. The shaded area shows statistically significant region (Fig. 4b). The domain chosen for this study lies mostly in the statistically significant area within the Indian region. This implies the model representation of the rainfall averaged over the grids over the MCR is quite close to that of that of the observational reanalysis. For further analysis, the

scatter plots between the all India rainfall and the rainfall over the MCR is examined for the simulation as well as for the observation. The correlation coefficient between the all India monsoonal rainfall and the rainfall over the MCR is compared for the model simulation and observational analysis (Fig. 4c). The correlation coefficient of the ISM rainfall and the rainfall over MCR during summer for

Table 2 Monsoon active spells

Year	Active_RCM4	Active_IMD
1989	17 Jul–20 Jul	21–24 Jul
	22 Jul–24 Jul	–
1990	–	22–24 Aug
1991	11–17 Jul	28–31 Jul
1992	09–15 Jul	26–29 Jul
	20–22 Jul	16–20 Aug
	29–31 Jul	–
1993	04–08 Jul	15–17 Jul
	03–05 Aug	–
1994	–	02–04 Jul
	–	09–16 Jul
1995	08–12 Jul	18–25 Jul
	19–24 Jul	–
1996	–	22–28 Jul
1997	–	30 Jul–01 Aug
	–	21–25 Aug
1998	01–05 Jul	03–05 Jul
1999	05–07 Jul	02–04 Aug
	11–13 Jul	07–09 Aug
	16–18 Jul	–
2000	08–10 Jul	12–14 Jul
	–	17–20 Jul
2001	31 Jul–03 Aug	09–12 Jul
2002	–	–
2003	03–18 Jul	23–28 Jul
	21–25 Aug	–
2004	14–16 Jul	30 Jul–01 Aug
	03–05 Aug	04–06 Aug
	–	08–12 Aug
2005	13–17 Jul	01–05 Jul
	25–28 Jul	25–29 Jul
	31 Jul–02 Aug	31 Jul–02 Aug

the model is 0.74 and 0.89 for IMD observation. The higher correlation between these dataset confirms that the region chosen by the study is a true representative of the all India summer monsoonal rainfall. Thus this representative region is taken for the detail study of the intraseasonal variability.

The monsoon is not uniform in terms of the daily rainfall; rather it shows temporal as well as spatial variations. Once the monsoon is established over India, there are times when the rainfall is very heavy for a long period and sometimes very less or no rain at all. The heavy rainfall spells during the monsoon period is called an active spell and dry spells are referred to as the break spells of ISM. Conventionally, the monsoon hits the Kerala coast on 1st June with a standard deviation of 8 days. It approximately takes 25 days to reach Delhi, Thus it is considered that from July

onwards whole country experiences the monsoonal rainfall. Similarly the retreat of monsoon starts from 1st September onwards from north India and completely retreats from India on 30th September. So July and August (JA) are the 2 months with maximum contribution of rainfall over India and also having monsoonal influence all over the Indian region. This is the reason why this study focuses on the rainfall of these 2 months for the study of intraseasonal variability of rainfall.

The model simulated and observed IMD daily rainfall time series is prepared by taking the area average rainfall over the MCR for JA months from 1989 to 2005. The daily standardized anomaly rainfall time series is prepared from the daily rainfall time series by dividing the daily precipitation anomaly with the standard deviation of the daily rainfall time series for both the model and IMD observation. The active and break spells are identified from this standardised anomaly rainfall time series. The active (break) spells as per definition are periods of high (low) precipitation. Thus active/break periods are defined as the periods where the standardize anomaly value of the rainfall is $+1/-1$ or more/less for at least three consecutive days in the standardised rainfall anomaly time series. The corresponding dates are termed as active and break spells for both model simulation and IMD observed value (same method used in Rajeevan study).

5 Active and break spells

Tables 2 and 3 show the active and break spells as identified by the definition above for the model and the IMD observation respectively for the period of simulation. The total numbers of active spells are 23 and 25 in model and observation respectively. The model simulation is lacking a single active spell during 1990,1994,1996,1997 and 2002 where as the analysis for IMD data shows at least one active period each year except for 2002. This particular year (2002) is a deficit monsoon year and is rightly captured by the model without any active spell of the rainfall. The simulated value for the average number of active days during JA is 6.2, which is close to the IMD observation of 6.3 days. The monthly distribution of the number of active days for the July and August are 5.3 and 0.9 for the model simulation, 4.5 and 1.8 for IMD observation respectively. Similarly, the standard deviation values for the active days are 5.8 and 3.5 for the simulation, and IMD observation respectively. The average number of active days is well represented in the model and is in close agreement with the IMD observation. The average numbers of active days are more in July as compare August. But in the model simulation, the number of active days is very high during July and very low during August as compare to the IMD

Table 3 Monsoon break spells

Years	Break_RCM4	Break_IMD
1989	09 Jul–14 Jul	30 Jul–03 Aug
	30 Jul–07 Aug	–
1990	07–09 Jul	–
	12–25 Jul	–
1991	01–07 Jul	01–04 Jul
	12–17 Aug	–
1992	02–06 Jul	03–10 Jul
1993	09–18 Aug	21–24 Jul
	–	08–13 Aug
	–	22–29 Aug
1994	22–26 Jul	–
1995	01–06 Jul	03–07 Jul
	–	13–16 Aug
1996	01–07 Jul	01–03 Jul
	11–13 Jul	–
1997	–	11–14 Jul
	01–04 Jul	–
	04–16 Aug	–
1998	–	21–26 Jul
	–	–
1999	03–06 Aug	01–05 Jul
	21–23 Aug	13–16 Aug
	–	–
2000	23–28 Jul	22–25 Jul
	–	01–07 Aug
2001	–	28–30 Aug
2002	09–14 Jul	03–14 Jul
	24–26 Jul	22–31 Jul
2003	–	–
	12–14 Aug	–
	28–31 Aug	–
2004	18–23 Jul	09–11 Jul
	25–31 Aug	20–22 Jul
	–	26–31 Aug
2005	07–12 Aug	08–14 Aug
	–	24–29 Aug

observed value. The higher value of the standard deviation for the simulation shows that the fluctuation from the average number of active days is more in the model simulation as compare to IMD observation. The total number of break spells in the model simulation and observation are 24 and 23 respectively. The model simulated average number of break days during JA is 8.6 days and 7.7 days for IMD observation. The analysis of monthly distribution of the break days shows the average number of break days for July and August are 5.7 and 2.9 in the simulation and 5.1 and 2.6 for IMD observation respectively. The standard

Table 4 Frequency distribution of the duration of Active spells in percent and its comparison with previous study

Spells	Model	IMD	Rajeevan et al. (2010)
3–4 days	65.2	64.0	79.0
5–6 days	21.7	24.0	12.0
7–8 days	8.7	12.0	6.0
9–10 days	0.0	0.0	3.0
>10 days	4.3	0.0	0.0

deviation values for the break days are 5.1 days for the simulation, 6.4 days for IMD observation. The simulated average number of break days is more in July than the August which is in close agreement with the IMD observation.

For the period of study (1989–2005) the models is in close agreement with the observation in representing the total and average number of active and break periods during JA. The average numbers of break days are more in comparison to that of the average number of active days. The frequency distribution of the active spells model and observation and their comparison with Rajeevan study is shown in Table 4. The simulation shows 65.2 % of the active periods have a life span of 3–4 days, whereas this category contributes 64 % in the IMD observation. The addition of the first and second categories i.e. the 3–4 days and 5–6 days together contribute close to 90 % of the active spell for both model and observation (as reported in Rajeevan study). Generally the active spells of longer duration (more than 7 days) contribute nearly 12 % in both model and observation. The active spell of more than 10 days is very rare (only 4.3 %) and the model rightly reproduce this feature. Similarly, Table 5 shows the frequency distribution of the break spells of model, observation and its comparison with previous studies. The contribution of 3–4 days spell (33.3 %) is less in the simulation as compare to the observed value (40–50), whereas the 4–5 days category has higher percentage in simulation (37.5 %) as compared to the observed value of (20–30 %). During break spells the contribution of 3–4 days and 5–6 days categories together is around 70 % of the total break spells for both model and observation (Also for the previous studies). The model nicely represents the frequency of the long break spells (7 days or more) which contributes around 30 %, and very close to the observed values and the previous studies.

The dates of the active and break spell of this study during the JA is not matching with the observation and the previous studies in most of the years. This mismatch in the dates with the previous studies may be attributed to the length of the study period considered in the present study and the methodology used to calculate the active/break spells. Because in earlier studies, researchers have considered the rainfall averaged over all Indian land points for

Table 5 Frequency distribution of the duration of break spells in percent and its comparison with previous study

Spells	Model	IMD	Rajeevan et al. (2010)	Gadgil and Joseph (2003)	Ramamurthy (1969) and De and Mukhopadhyaya (2002)
3–4 days	33.3	45.8	40.0	44.8	49.5
5–6 days	37.5	29.1	28.0	22.8	19.8
7–8 days	12.5	16.7	19.0	14.3	16.2
9–10 days	4.2	4.1	3.0	6.7	6.3
>10 days	12.5	4.2	10.0	11.4	8.2

4 months (entire monsoon period, JJAS), whereas in the present study, the rainfall is considered over the representative MCR only for JA. The mismatch of the active/break spells of the model with the observation of the present study may be due to the following two reasons (although the length of period and methodology used are same). First, a two tailed student's t test for JA is carried out for the model and the IMD data set at 95 % confidence level. This plot (figure not shown) suggests that most of the area under the MCR is not statistically significant. This means that the model representation of the rainfall averaged over the grids over MCR during JA is showing deviation as compare to the observational reanalysis. Secondly the Taylor diagram is plotted between the JJAS precipitation of the model with respect to the IMD observation and the ERA-Int reanalysis (Fig. 4d). The JJAS rain of the model in neither well correlated neither with the IMD observation nor with the ERA-Int reanalysis, the correlation co-efficient are close to zero for both ERA-Int and IMD with respect to model output. The low correlation of the model precipitation with the reanalysis implies that the reanalysis has very less influence in determining the variability while the model processes plays the dominant role in deciding the interannual variability of the monsoon (Maharana and Dimri 2014b). Because of the above two reasons the dates of the active and break spells of the simulations are not matching with the corresponding observation.

6 Evolution of active and break phase

This section mainly deals with the evolution of active and breaks phases using the lagged composite of different meteorological parameters. The composite analysis is done to make sure that the mean atmospheric condition is represented. The daily data of various parameters are used to analyze the -12 to $+12$ lagged phase. The lag00 phase is chosen as the composite of the middle date of the active and break phases. Here the propagation characteristic is studied only over the Indian land points to analyse the specific characteristics of the active/break phases with special focus on the MCR. Figure 5a, b show the evolution of active phase in term of lagged daily rainfall anomaly in

IMD observation and corresponding model output respectively. The lag-12 phase of the composite rainfall anomaly shows that the MCR has negative rainfall anomaly and southern India has a positive rainfall anomaly (Fig. 5a). As the time approach towards lag00 time, the positive band of the rainfall anomaly moves north and northwest direction and occupies the MCR, which implies that the rainfall is very high over this region. The foothill of Himalayas and the southern peninsular region are showing the negative anomaly of rainfall. This particular phenomenon is the characteristic feature of the active phase of the ISM. Since the active phases mostly last for 3–4 days, so the north and northwest movement of the positive rainfall anomaly from the BoB towards the northwest part of India are predominant from lag -02 to lag $+02$ phases. From lag $+02$ onwards the movement of the positive anomaly towards the north and northwest direction occur and in the next 12 days the MCR is occupied by the negative anomaly of the rainfall. The model is able to reproduce the evolution of the active days and the north and northwest propagation of the positive rainfall anomaly in most of the lagged phases (Fig. 5b). Figure 6a, b depicts the lagged composite of the vertical integrated moisture and transport for the ERA-In observation and simulation for the active phase respectively. Prior to the active phase cyclonic anomalies form over BoB and it moves northwest towards the MCR. It starts to appear over north BoB during lag -04 phase and moves towards the land and dissipate after lag $+02$ phases over the western India. During the onset of active period the convergence occurs over the MCR and the moisture is transported to this region from the zone of divergence i.e. BOB and the Arabian Sea. The cyclonic anomaly over the MCR signifies intense convergence is taking place over this region (Fig. 6a). The model shows cyclonic anomaly over the India exists prior to the active phase. The convergence due to the cyclonic anomaly increases during lag -02 to lag $+02$ phases i.e. during the active period over the MCR which results in heavy precipitation over MCR. The model nicely represents the composite of vertical integrated moisture flux over the Indian region, the divergence zone of moisture over the Arabian Sea and BoB, transport of the moisture into the MCR and the vortex over the MCR for most lagged phases (Fig. 6b).

Fig. 5 a, b The lagged rainfall (mm; *shaded*) composite of the active spell of the IMD and model

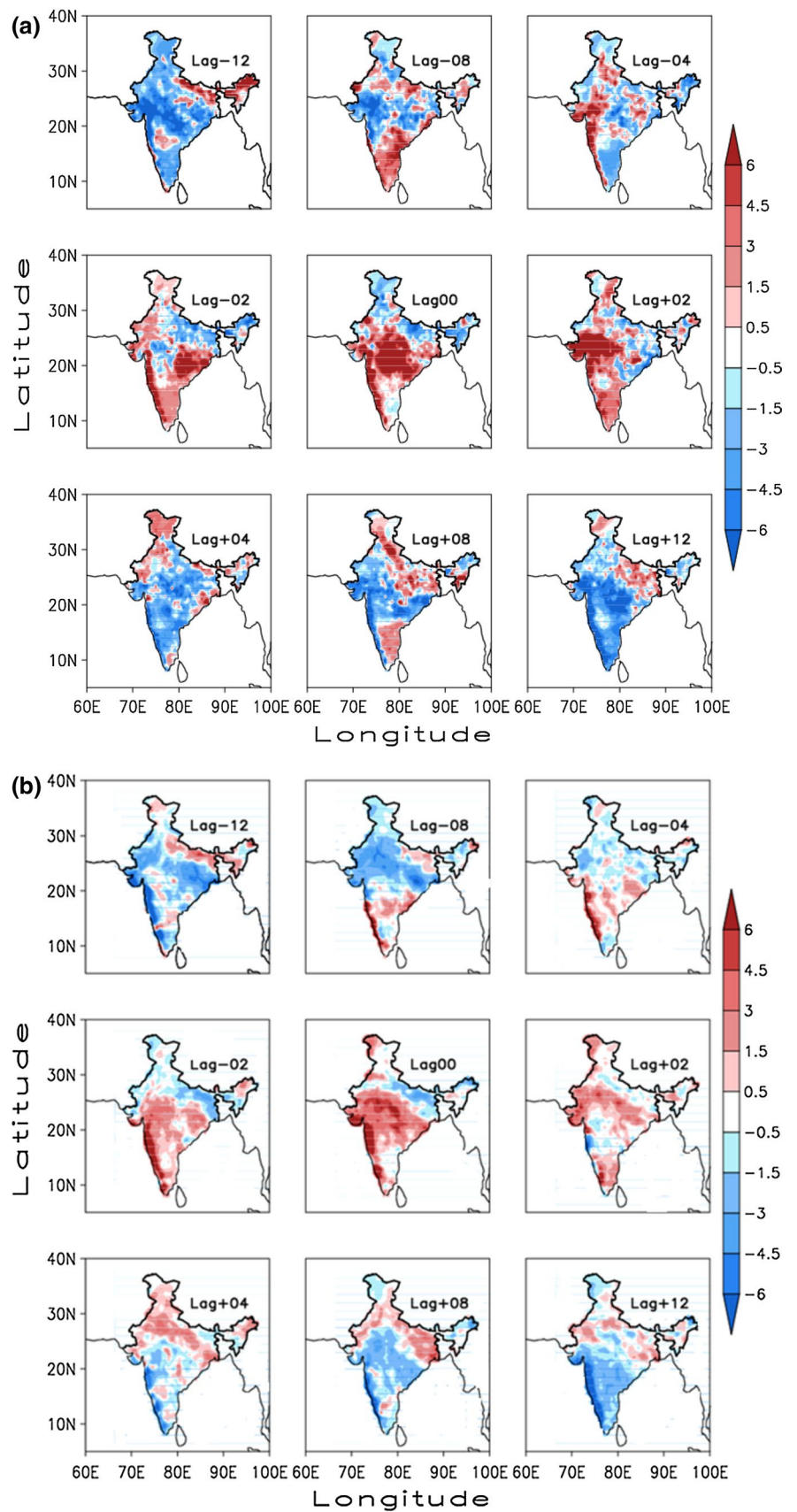


Fig. 6 a, b Same as Fig. 5a, b, but for vertical integrated moisture flux (Kg/m/s ; shaded) and transport ($\times 10^4 \text{ mm}$; vector)

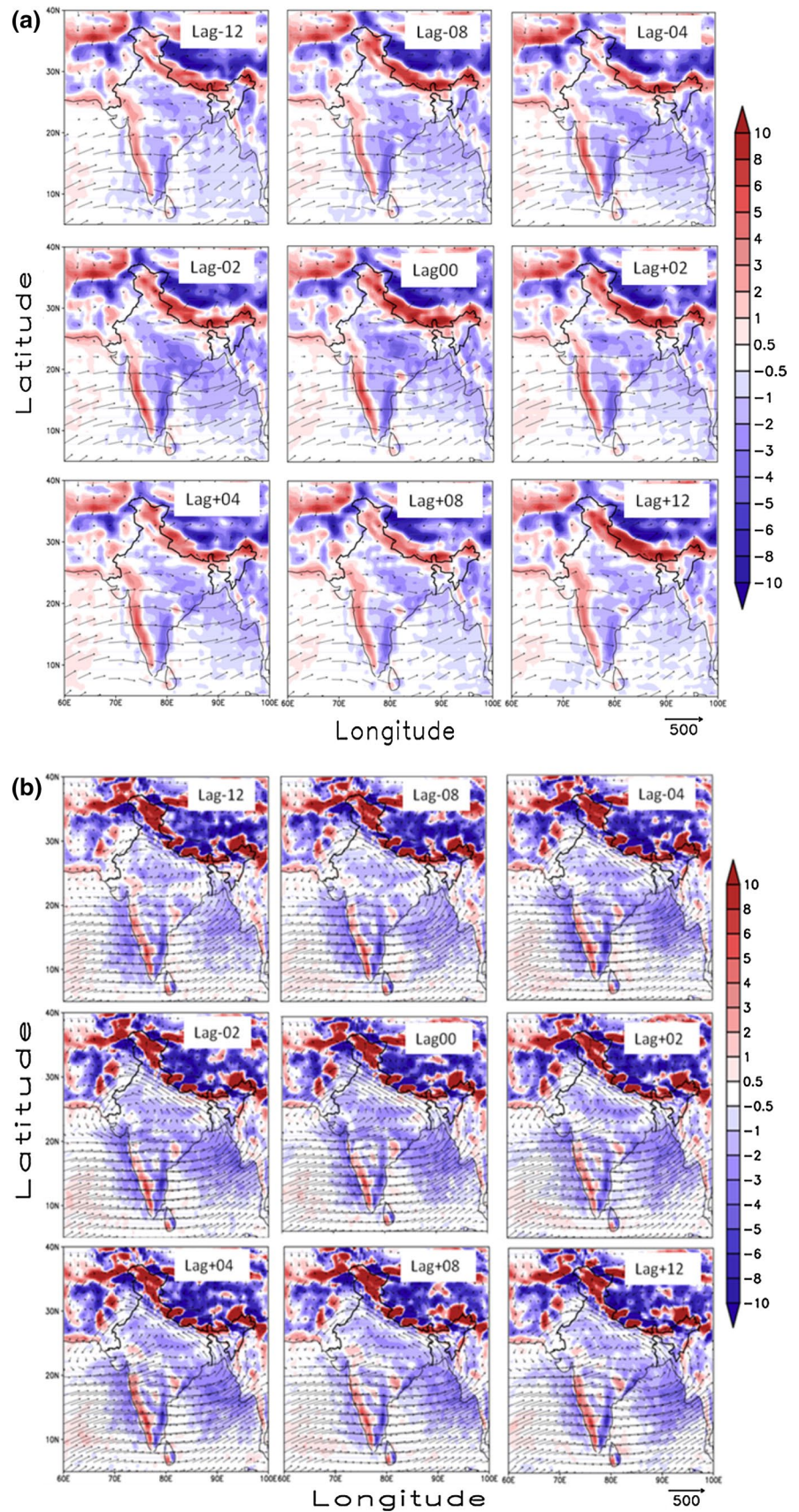


Figure 7a, b represents the lagged composite of the daily rainfall anomaly to show the evolution of break phase over the MCR for IMD observation and model respectively. The composite of IMD observation shows a positive anomaly of rainfall over MCR and negative rainfall anomaly over south India during lag -12 . As the time approach towards the lag00 phase, the negative rainfall anomaly moves north and northwest ward to occupy the MCR. The positive anomaly of rainfall appears from lag $+02$ phase in the southern Indian region which gradually moves north and northwest direction and occupy the MCR during lag $+12$ phase. The composite of the model is in agreement with the IMD observation of the present study; it captures the observation in all the lagged phases, the evolution and the revival of active phase from break phase (Fig. 7b). The average life span of most of the break period is 4–5 days which is more than the average life of active period. This can be inferred from the composite plots, where the negative rainfall anomaly starts to appear over the south and east of India (originated over BoB) and starts to move northwest direction and occupy the MCR during lag00 phase. It moves further northwest and completely disappears in the lag $+04$ phases. This phenomenon is nicely represented by the model and is in good agreement with the corresponding observed value. Figure (8a, b) explains the lagged composite of vertical integrated moisture flux and transport for break period and its evolution for ERA-In observation and model. The observed vertical integrated moisture flux (Fig. 8a) shows a weak cyclonic anomaly over the BoB close to the West-Bengal coast in the lag -12 to lag -08 phases. As the break period approaches the cyclonic anomaly over that region disappear from lag -04 to lag $+02$ phases and hence the area of convergence over the over the MCR is very weak. The area over the Arabian Sea and northwest region of India shows a divergence of wind and the moisture is transported away from these regions and moves towards the foot hills of Himalayas. So the rainfall decreases over MCR and increase over the foot hills of Himalayas during break period. These are the main features of the break spell during ISM. After the break spell, the cyclonic anomaly again reappears from lag $+04$ phase onwards over north BOB. The model also captures the cyclonic anomaly in the lag -12 and lag -08 phases (Fig. 8b). The core of the cyclonic anomaly shows a northwest shift in the model and is found over the western part of India. The cyclonic anomaly weakens with the commencement of the break phase (From lag -04 to lag $+02$) and the moisture is transported away from the MCR region during this period towards the foothills of Himalayas. The model rightly captures the zones of divergence of moisture and its transport away from the MCR towards the foot hills of Himalayas during break period.

This study shows that the revival from the break/active to active/break period occurs by the northward propagation of the positive/negative rainfall anomaly band. This is captured by the model and also in agreement with the previous study (Lawrence and Webster 2000). The major feature of the active and break spell, i.e. the rainfall anomaly over MCR and the opposite sign of the same in the foothill of the Himalayas and the southern India are nicely represented.

This section deals with the different propagation characteristics associated with the monsoon breaks over the domain of simulation including the land and oceanic region. The earlier analysis of the pentads deals with the propagation characteristics over the Indian land points only and more concerned over the rainfall anomalies over MCR and foothill of Himalayas. Here, the time sequence of composite anomalies of the triads is analyzed which simultaneously shows the origin and propagation of different type of anomalies over the whole domain of simulation during ISM. Also, the results are compared with previous studies to get a better understanding of the propagation phenomena. The methodology to calculate the triad is adopted from Krishnan et al. (2000) but is prepared for the precipitation over the domain of simulation. The triad0 refers to the average of composite anomaly over (day -1 , day 0 and day $+1$), which is the onset of the break period. Similarly the other triads are calculated for following and preceding days of the onset of break (Fig. 9). Prior to the onset of break period, a band of positive rainfall anomaly is seen spreading over the BoB to northwest India in the triad-4 to triad-2. But in triad-2 to triad0, the development of the negative rainfall anomaly starts over BoB. The higher precipitation due to the convective activity over the land may cause suppress convection or negative rainfall anomaly over BoB. Beside that a negative rainfall anomaly starts to appear over the Arabian Sea (during triad-4 and triad-3) and its subsequent movement towards east (triad-1) also causes the negative rainfall anomaly to develop over BoB. The onset of the break phase (triad-1 and triad0) takes place by the northwest movement of the negative rainfall anomaly from BoB towards the northwest India. And its life span is around 4–5 days, where as the eastward propagating negative anomaly from the Arabian Sea show no significant eastward movement during this period. The eastward propagating negative rainfall anomaly gets decoupled from the anomaly moving towards the northwest direction. The eastward moving negative rainfall anomaly cause less precipitation over the south-east Asia for a week after the onset of break period. With the onset of the break period, a positive band rainfall anomaly appear over the BoB and southeast Asia and cause heavy precipitation over these regions. The weakening of the heavy precipitation over MCR starts 1 week prior to the

Fig. 7 a, b The lagged rainfall (mm; *shaded*) composite of the break spell of the IMD and model

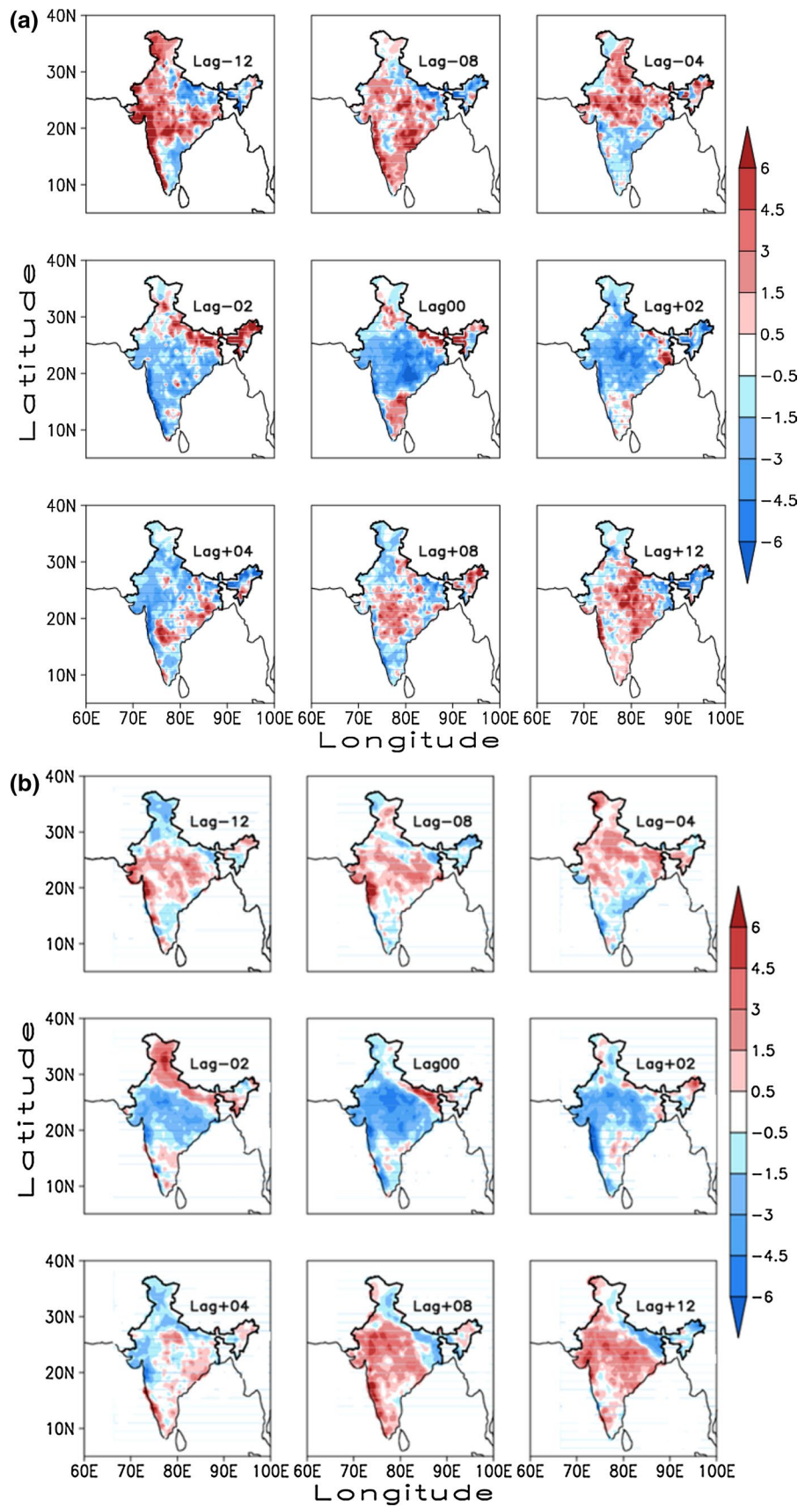
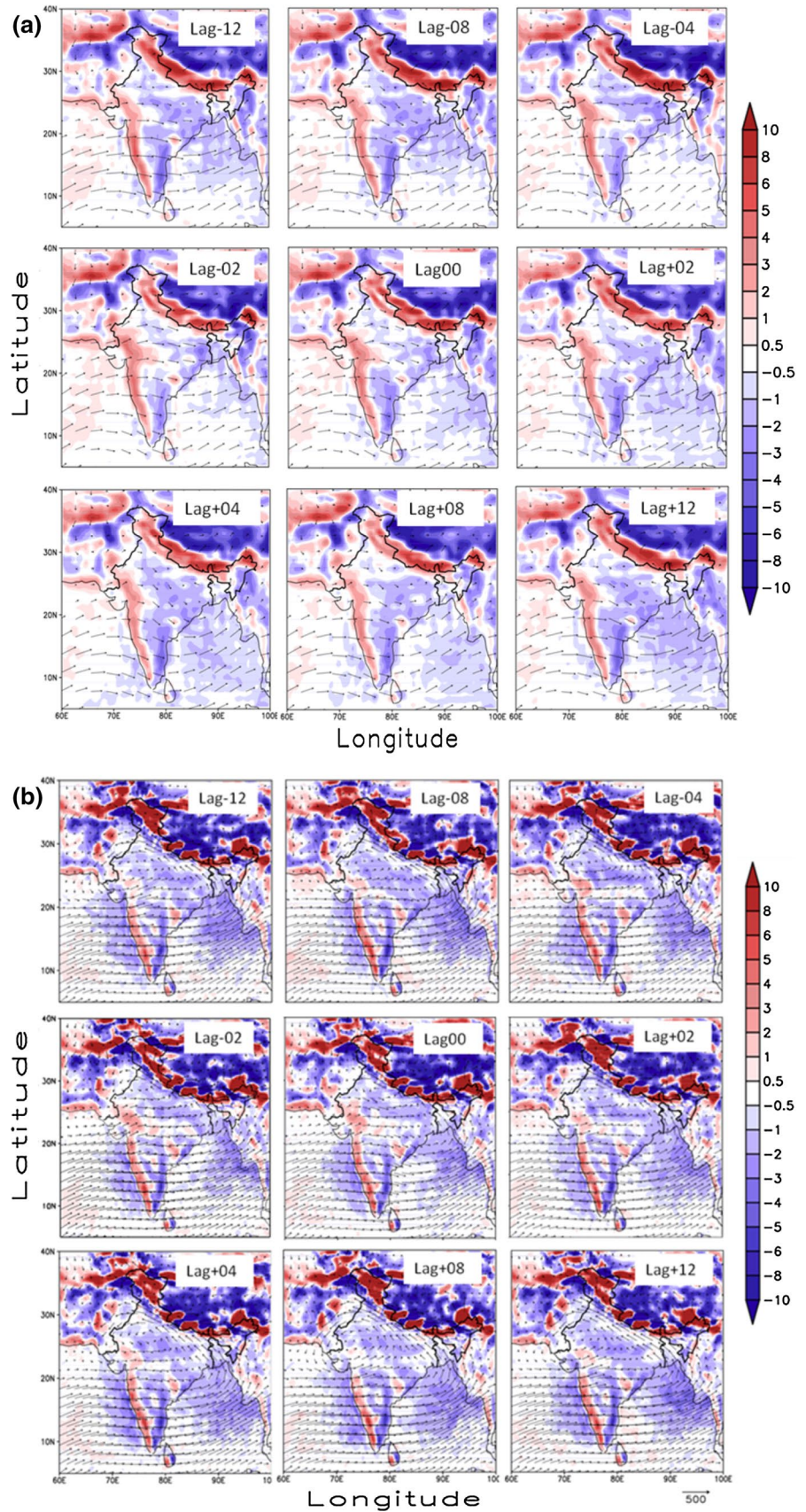


Fig. 8 a, b Same as Fig. 7a, b but for vertical integrated moisture flux (Kg/m/s ; *shaded*) and transport ($\times 10^4 \text{ mm}$; vector)



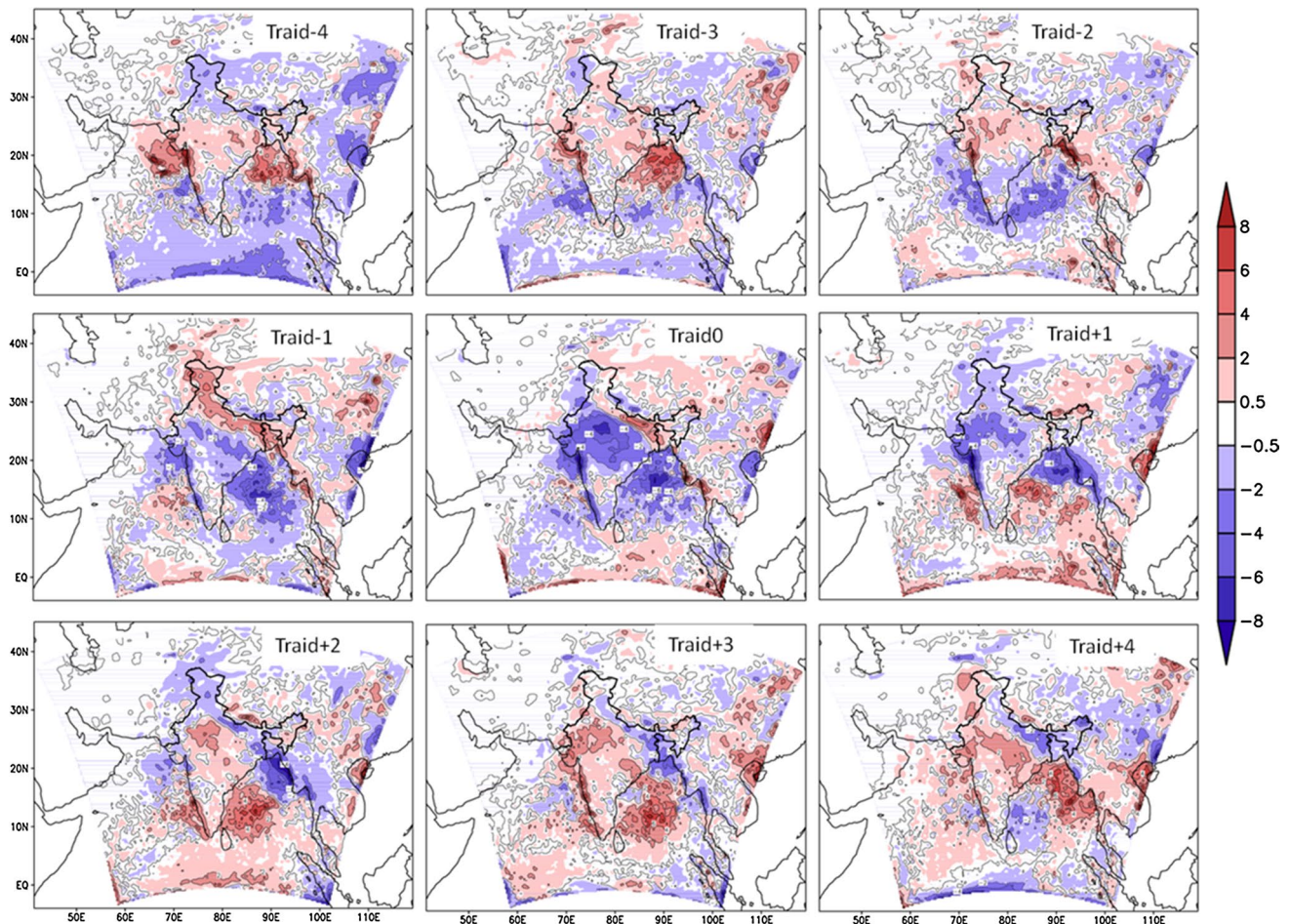


Fig. 9 Depicts the sequence of composite rainfall anomaly triads (*shaded*) and evolution of break spell and different propagation

onset of the break spell as the negative rainfall anomaly are started to build over the Arabian sea and its progressive eastward movement. Similar results were reported by Krishnan et al. (2000) using OLR composite anomaly. Chang (1977) shows the interaction between the low latitude wave dynamics and tropical convective heating can excite the equatorial Kelvin wave. The eastward propagation can be partly be explained by the Kelvin wave, such as the 40–50 days Madden-Julian oscillation (Madden and Julian 1971, 1972). Similarly Krishnan et al. (2000) through various modelling experiment explained the north-northwest propagation of the negative precipitation anomaly attributed to the northwest propagation of the Rossby waves which are generated in response to the non-convective/negative precipitation anomaly over the BoB. So the model shows some shades of its ability to reproduce the quasi-biweekly oscillation which is related to the northward propagation and the 40–50 days eastward moving Madden-Julian oscillation. But further investigation need to be done for the confirmation of these propagations.

7 The intense long break and heat trough type meridional circulation

During ISM period, the temperature is very high over the north-western part of the Indian land mass (Fig. 2a). A low pressure region develops over the surface as compare to the seas (figure not shown), which results in establishment of a well defined heat low (trough) type circulation over this region. The heat trough type circulation doesn't allow more rainfall to occur and hence the rainfall over the northwest part of India (over Rajasthan region) is very less. In an earlier study, Raghavan (1973) has described the heat trough type circulation during the monsoon period. During the long break period the surface temperature rises (more as compare to the active period) and heat trough type circulation established over the India region where monsoon trough acts. Rajeevan study uses NCEP daily meridional wind to study this phenomenon and suggested that further analysis is to be done for better understanding of the heat trough type circulation. So the model output has been

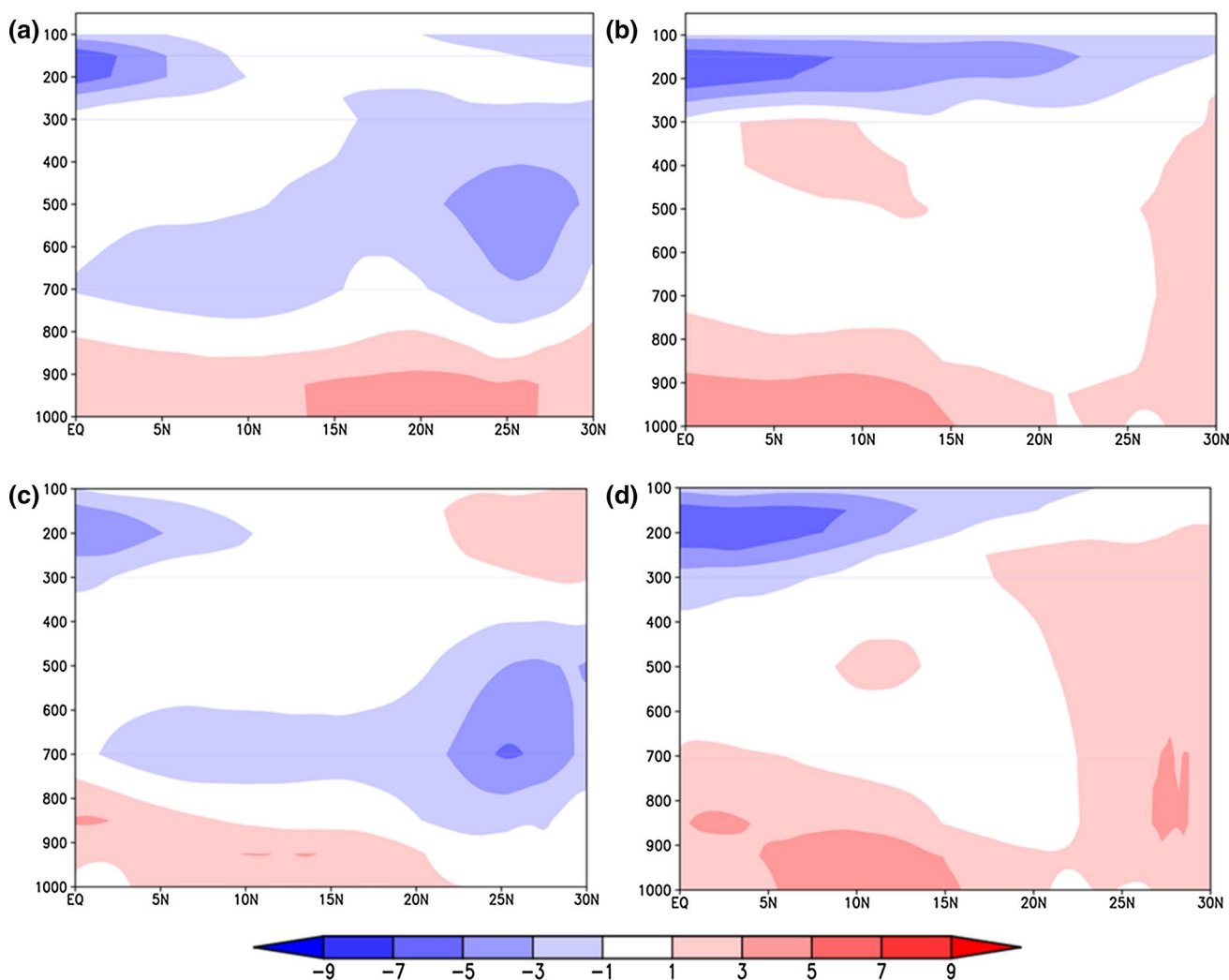


Fig. 10 Latitude-Height section of meridional wind climatology (m/s; shaded) during July averaged over 65° – 70° E (a, c) and over 78° – 88° E (b, d). The figures in the first row represent the ERA-Int observation and the second row represents the model output

analyzed in this section to study the heat trough type circulation and associated phenomena.

Figure 10a, b) show the latitude-pressure section of meridional wind climatology (m/s) during July averaged over 65° – 70° E (eastern) and over 78° – 88° E (western) for the ERA-Int observation and Fig. 10c, d) are the same but for the model simulation respectively. The vertical profile of the mean July meridional circulation over western region of India (65° – 70° E) is associated with a shallow cell and the convergence is restricted to the 800 hPa and the strong northerly around 700 hPa which doesn't allow the upward movement of the moisture or convection. So this results in low precipitation over this region. Similarly, over the eastern part of India (78° – 88° E), the northerly are found over 300 hPa. So the vertical movement of the moisture laden air (convection) is not restricted as it condenses at certain height and falls as precipitation and hence more

precipitation over this region (Fig. 10a, b). Similar results were reported in Rajeevan study. In the western region the model realistically simulates the strong northerly at the 700 hPa which restrict the upward motion of moisture (Fig. 10c). The simulation over eastern part shows that the northerly lies in the 300 hPa and the extent of the moisture containing southerly is very high which results in heavy precipitation over this region (Fig. 10d). The mean meridional wind during July over eastern as well as western region of India is well captured in the model. For further analysis, the composite of the entire active and break spells identified in this study are analysed over MCR to establish the mean atmospheric condition during the active or break spells. The composite of the latitude-pressure section of mean meridional wind (m/s) averaged over 78° – 88° E (Over MCR) of all the active spells for observation and model are shown in Fig. 11a, b. The analysis of the composite of observations

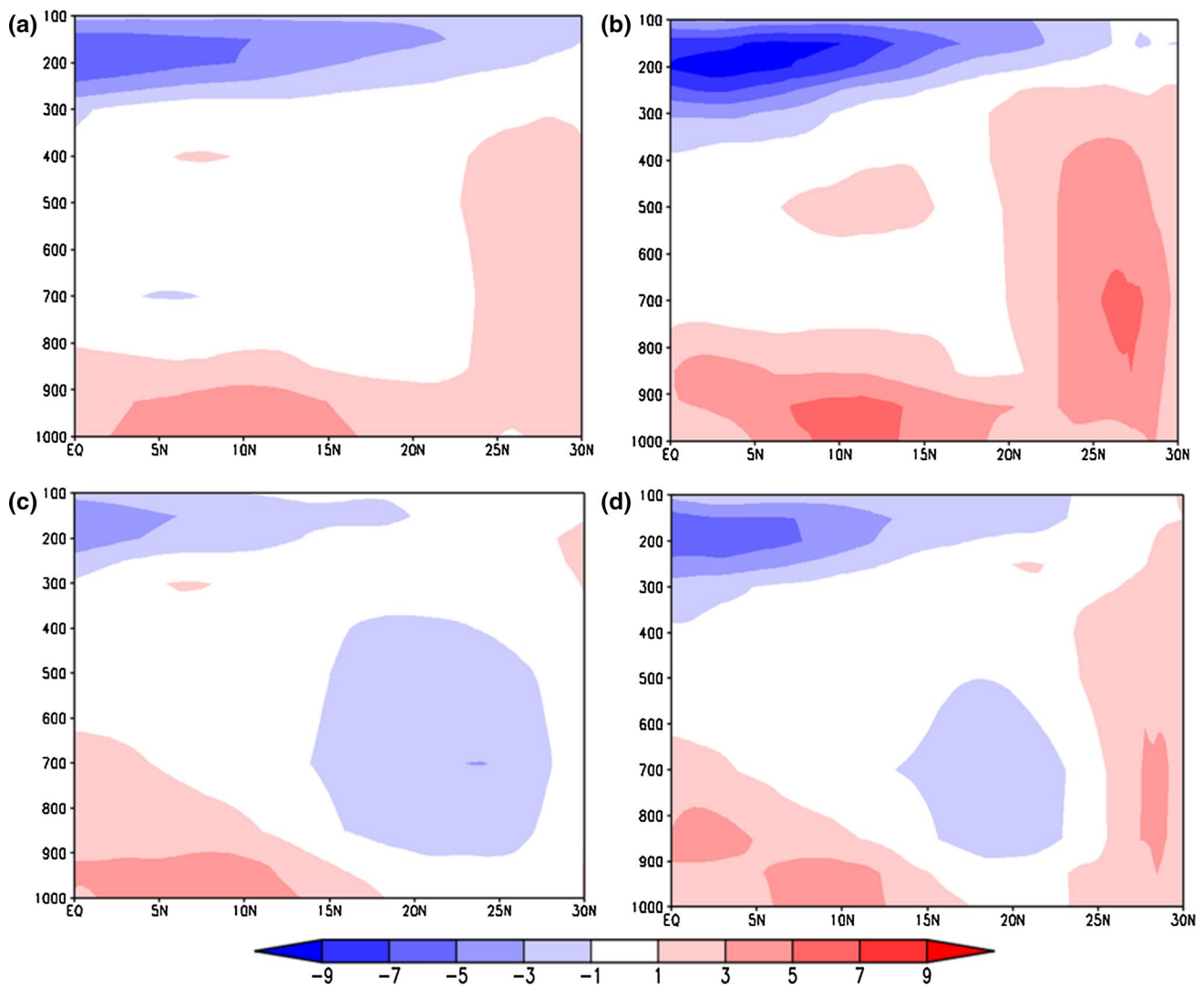


Fig. 11 a, b The latitude-pressure section of mean meridional wind (m/s; *shaded*) averaged over 78°–88°E for composite of all active period for ERA-Int observation and model. Similarly **c, d** show the

latitude-pressure section of mean meridional wind (m/s) averaged over 78°–88°E for composite of all break period for ERA-Int observation and model

shows that the strong northerly lies over 300 hPa, whereas the extent of the strong southerly is up to 300 hPa. So southerly carrying the moisture doesn't have any obstacle in the atmosphere over MCR. This kind of circulation is similar to the mean circulation which prevails over eastern India during July. This circulation supports heavy rainfall over MCR during active spells. The model nicely reproduces the above phenomenon by capturing the strength and position of the southerly wind. Similar analysis of the composite of the break period in ERA-Int observation over MCR shows that the strong northerly exists at 700 hPa which doesn't allow the vertical movement and cause restriction in the precipitation spells (Fig. 11c). Whereas the model shows the weaker northerly in the 700 hPa region having less spatial extent, which hinders the rainfall over the MCR during

break period (Fig. 11d). This circulation resembles the mean meridional circulation during July over the western India or the heat trough type circulation. This type of circulation restricts the upward movement of the moisture or convection resulting in less precipitation. So the rainfall is very less over MCR during the break periods. So the major findings of this section are the mean atmospheric conditions during the active phase of the ISM over MCR are similar to the atmospheric conditions prevailing over eastern India which supports heavy rainfall and during the break period the atmospheric conditions over the MCR resemble the atmospheric conditions over western India (Rajasthan) or heat trough type circulation which does not allow much rainfall to occur.

In this section, the relation between the availability of moisture and the precipitation pattern over the MCR during

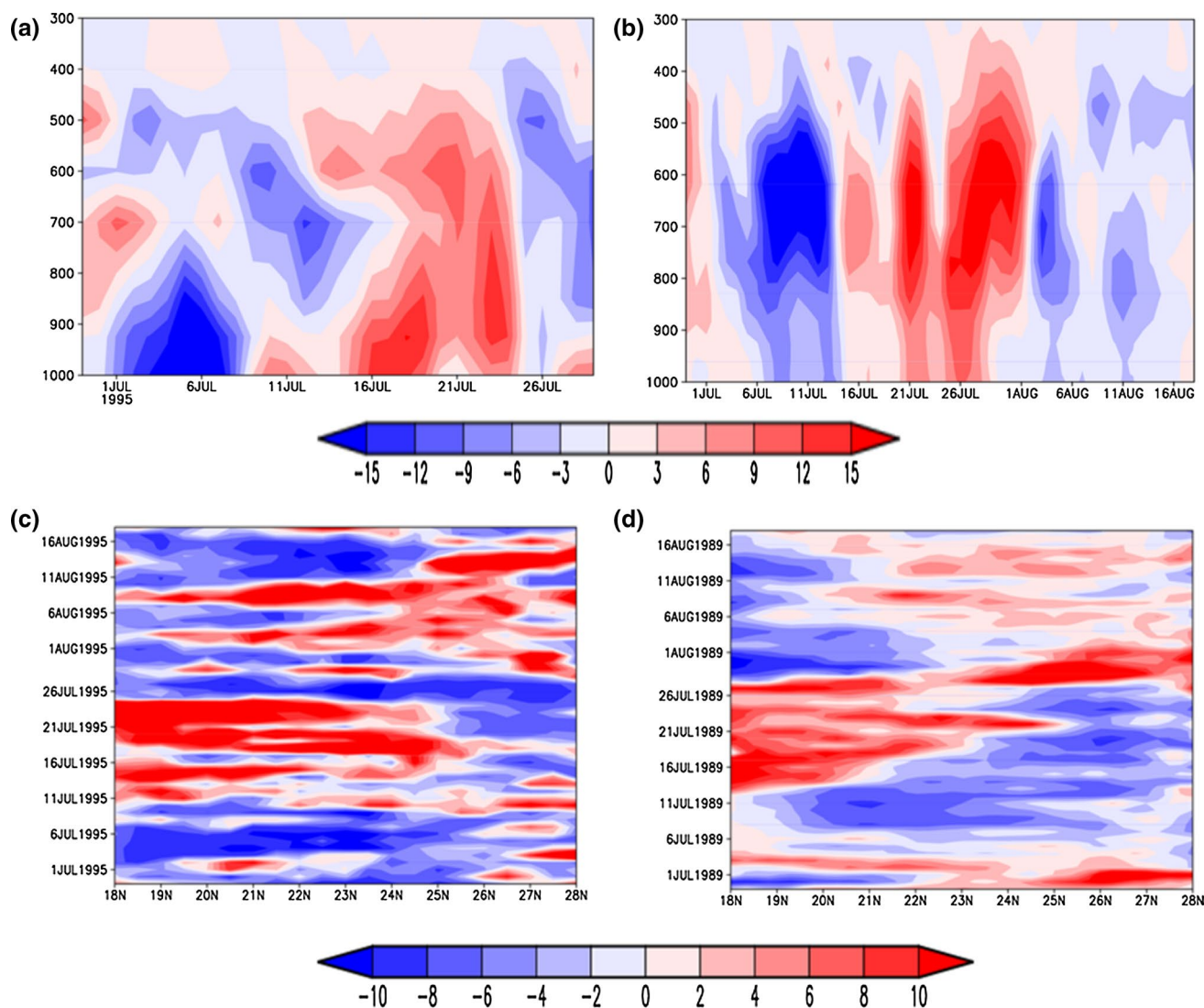


Fig. 12 **a, b** The time-pressure plot of specific humidity averaged over the latitude of MCR for the observation (1995) and model (1989) respectively. Similarly **c, d** represents the time-latitude plot of precipitation averaged over the longitude of MCR for the observa-

tion (1995) and model (1989) respectively. The active period in the observation is 18–25 July and break period is 03–07 July. Similarly the active periods in the model are 17–20 July and 22–24 July. The break spells are 09–14 July and 30 July–07 August

active and break periods are analyzed (The active period in the observation is 18–25 July and break period is 03–07 July of 1995. Similarly the active periods in the model are 17–20 July and 22–24 July and the break spells are 09–14 July and 30 July–07 August of 1989). The above mentioned active and break days are chosen to show the transition of moisture and precipitation over MCR during break to active period (Fig. 12a–d). The availability of moisture during the active spells is very high, because the convergence of the moisture laden air over the MCR during the active periods (Fig. 6). The observational analysis shows the transition of moisture availability over the MCR from the break to active period (Fig. 12a). The model rightly captures the availability of the moisture and its transition over the MCR at different

spells (Fig. 12b). The availability of the moisture over the MCR is very high during the active period and the vertical extent is up to 400 hPa whereas the moisture availability is relatively less during the break period. The similar patterns are also found in the model, in relation to the spatial structure of moisture availability and the active/break over MCR. The moisture availability and the precipitation over the MCR is also compared (Fig. 12c, d). This shows that the precipitation over MCR depends upon the available moisture over this region; the precipitation is more during active period i.e. during the period when the moisture availability is more over MCR and vice versa for break period. This plot also shows the northward propagation of the rainfall which revives the active phase from break phase over the MCR.

8 Summary and conclusion

The study aims to examine the intraseasonal variation of rainfall and associated atmospheric processes over a representative zone over India during monsoon using a RCM. The student's *t*-test and the scatter plot shows that the MCR is a true representative for the all India rainfall, and the daily rainfall over this region can be taken further for the analysis of active and break spells. The active and break spells are determined during JA for both the model simulation and IMD observation. The mismatch in the active and break spells of the present study with previous studies may be attributed to the differences in the length of the study period and the different methodologies used to identify the spells. In this study the daily rainfall over the MCR is considered, whereas the earlier studies consider the daily all India rainfall. The mismatch between the model and the IMD observed data (although the study period and methodology are same) is explained by the *t* test at 95 % confidence level between model and observation for JA precipitation. It reveals that the model is not well co-related with the observation rainfall over MCR during these 2 months. This may be the possible reason why the dates of the active and break spells are different in the model and observational data sets. Also, the analysis of Taylor diagram reveals that the JJAS rainfall is not well correlated with the ERA-In observation. This means model processes and physics play dominant role in defining the variability and ERA-In reanalysis has very less role in it. The frequency distribution shows 3–4 days category contributes maximum to the total active spells and the 3–4 and 5–6 days categories together contribute more to the break spell for both model and simulation. The model able to rightly represents the percentage contribution of the different category of the rainfall spells during active and break period. The study reveals that the in the model environment the short spell of break period (3–4 days) are decreasing but the moderate long spells (5–6 days) are increasing in the present period. The analysis of the lagged composite rainfall anomaly nicely represents the major features of the active/break i.e. the positive/negative rainfall anomaly over MCR and negative/positive rainfall anomaly over foothills of Himalayas and south India. Also, the model accurately simulates the evolution of active and break spell over MCR, i.e. the transition of the active/break phase to break/active by the northward movement of the band of positive/negative rainfall anomaly over India. The moisture source during the active and break spells, the transport of the moisture towards MCR during active spells and the transport of the moisture away from the MCR during break spells are nicely represented in the simulation with spatial accuracy. The model shows some tendency to realistically represent the eastward and the

northward propagations. The comparison with the earlier studies shows that, this eastward and northward propagation may be related to the excitement of the Kelvin wave and Rossby wave respectively. But further study need to be done for the confirmation of these facts. During intense break, the rising temperature causes a heat trough type circulation over MCR. The model nicely represents the heat trough type circulation over the western India which denies heavy rainfall and the moist convective regime over the eastern India which supports the heavy rainfall. This study confirms that the mean atmospheric condition during the active phase over MCR is similar to the atmospheric condition prevail over eastern India and during break period the atmospheric condition over the MCR resembles the atmospheric condition over western India or heat trough type circulation. The process associated with the moisture–precipitation relation during the active and break phase and their transition is also examined. The discussion above implies that the model is showing robust skills in capturing the intraseasonal variability and importantly the physical processes associated with active and break spells. The study of different intraseasonal oscillation of rainfall associated with ISM over India and their relation with the excitation of the kelvin and Rossby wave using the regional climate model will be done in the future.

Conflict of interest None.

References

- Abhik S, Mukhopadhyay P, Goswami BN (2013) Evaluation of mean and intraseasonal variability of Indian summer monsoon simulation in ECHAM5: identification of possible source of bias. *Clim Dyn* 43:389–406
- Achuthavarier D, Krishnamurthy V (2009) COLA technical report 285
- Ajayamohan RS (2007) Simulation of South-Asian Summer monsoon in a GCM. *Pure appl Geophys* 164:2117–2140
- Ajayamohan RS, Goswami BN (2007) Dependence of simulation of boreal summer tropical intraseasonal oscillations on the simulation of seasonal mean. *J Atmos Sci* 64(2):60–478
- Bhaskaran B, Murphy JM, Jones RG (1998) Intraseasonal oscillation in the Indian summer monsoon simulated by global and nested regional climate models. *Mon Wea Rev* 126(12):3124–3134
- Bhate J, Unnikrishnan CK, Rajeevan M (2012) Regional climate model simulations of the 2009 Indian summer monsoon, Indian. *IJRPS* 41(4):488–500
- Chang CP (1977) Viscous internal gravity waves and low-frequency oscillations in the tropics. *J Atmos Sci* 34(6):901–910
- Chen T, Chen J (1993) The 10-20-Day model of the Indian monsoon: its relation with the time variation of monsoon rainfall. *Mon Wea Rev* 121:2465–2482
- De US, Mukhopadhyay RK (2002) Break in monsoon and related precursors. *Mausam* 53:09–318
- Dee DP et al (2011) The ERA-Interim reanalysis: configuration and performance of the data assimilation system. *QJR Meteorol Soc* 137:553–597

- Dickinson RE, Henderson-Sellers A, Kennedy PJ (1993) Biosphere-atmosphere transfer scheme (bats) version 1e as coupled to the NCAR community climate model. Tech rep National Center for Atmospheric Research
- Fritsch JM, Chappell CF (1980) Numerical prediction of convectively driven mesoscale pressure systems. Part I: Convective parameterization. *J Atmos Sci* 37:1722–1733
- Fu X, Wang B, Li T (2002) Impacts of air-sea coupling on the simulation of mean asian summer monsoon in the ECHAM4 model. *Mon Wea Rev* 130(12):2889–2904
- Gadgil S, Joseph PV (2003) On breaks of the Indian monsoon. *Proc Indian Acad Sci (Earth Planet Sci)* 112:529–558
- Giorgi F, Coppola E et al (2012) RegCM4: model description and preliminary tests over the multiple cordex domain. *Clim Res* 52:7–29
- Goswami BN, Ajaya Mohan RS (2001) Intraseasonal oscillations and interannual variability of the Indian summer monsoon. *J Clim* 14:1180–1198
- Goswami BN, Xavier PK (2005) Dynamics of “internal” interannual variability of the Indian summer monsoon in a GCM. *J Geophys Res Atmos* 110(D24):1984–2012
- Goswami BN, Ajayamohan RS, Suresh Kumar G (1998) Intraseasonal oscillations and interannual variability of surface wind over the Indian monsoon region. *Proc Indian Acad Sci (Earth Planet Sci)* 107:4–64
- Goswami BN, Venugopal V, Sengupta D, Madhusoodan MS, Xavier PK (2006a) Increasing trends of extreme rain events over India in a warming environment. *Science* 314:1442–1445
- Goswami BN, Wu G, Yasunari T (2006b) The annual cycle. Intraseasonal oscillations and road block to seasonal predictability of the Asian summer monsoon. *J Clim* 19:5078–5099
- Goswami BB, Mukhopadhyay P, Khairoutdinov M, Goswami BN (2012) Simulation of Indian summer intraseasonal oscillations in a superparameterized coupled climate model: need to improve the embedded cloud resolving model. *Clim Dyn* 41:1497–1507
- Grell AG (1991) Prognostic evaluation of assumptions used by cumulus parameterizations. *Mon Wea Rev* 121:764–787
- Grell AG, Dudhia J, Stauffer DR (1994) A description of the fifth-generation Penn State/NCAR mesoscale model (MM5). Technical Note NCAR/TN-398+STR, 121p
- Halder M, Mukhopadhyay P, Halder S (2012) Study of the microphysical properties associated with the Monsoon Intraseasonal Oscillation as seen from the TRMM observations. *Ann geophys* 30(6):897–910
- Hartmann DL, Michelsen ML (1989) Intraseasonal periodicities in Indian rainfall. *J Atmos Sci* 46:2838–2862
- Holtlag AAM, Boville BA (1993) Local versus nonlocal boundary-layer diffusion in a global climate model. *J Clim* 6:1825–1842
- Hoyos CD, Webster PJ (2007) The role of intraseasonal variability in the nature of Asian monsoon precipitation. *J Clim* 20:4402–4423
- Jones RG, Murphy JM, Noguer M (1995) Simulation of climate change over Europe using a nested regional-climate model. I: assessment of control climate, including sensitivity to location of lateral boundaries. *QJR Met Soc* 121:1413–1449
- Kang IS, Jin K, Wang B, Lau KM, Shukla J, Krishnamurthy V, Liu Y (2002) Intercomparison of the climatological variations of Asian summer monsoon precipitation simulated by 10 GCMs. *Clim Dyn* 19:383–395
- Kiehl JT, Hack JJ, Bonan GB, Boville BA, Breigleb BP, Williamson D, Rasch P (1996) Description of the NCAR community climate model (CCM3). Tech. Rep. NCAR/TN-420+STR, National Center for Atmospheric Research
- Klingaman NP, Weller H, Slingo JM, Inness PM (2008) The intraseasonal variability of the Indian summer monsoon using TMI sea surface temperatures and ECMWF reanalysis. *J Clim* 21:2519–2539
- Kripalani RH, Kulkarni A, Sabade SS, Revadekar JV, Patwardhan SK, Kulkarni JR (2004) Intra-seasonal oscillations during monsoon 2002 and 2003. *Curr Sci* 87:325–331
- Krishnamurthy V, Shukla J (2000) Intraseasonal and interannual variability of rainfall over India. *J Clim* 13:4366–4377
- Krishnamurthy V, Shukla J (2007) Intraseasonal and seasonally persisting patterns of Indian monsoon rainfall. *J Clim* 20:3–20
- Krishnan R, Zhang C, Sugi M (2000) Dynamics of breaks in the Indian summer monsoon. *J Atmos Sci* 57:1354–1372
- Kulkarni A, Sabade SS, Kripalani RH (2006) Intra-seasonal Variations of the Indian Summer Monsoon Rainfall. Indian Institute of Tropical Meteorology RR114
- Lal M, Meehl GA, Arblaster JM (2000) Simulation of Indian summer monsoon rainfall and its intraseasonal variability in the NCAR climate system model. *Reg Environ Change* 1:163–179
- Lawrence DM, Webster PJ (2000) Interannual variation of the intraseasonal oscillation in the south asian summer monsoon region. *J Clim* 14:2910–2922
- Madden RA, Julian PR (1971) Detection of a 40–50 day oscillation in the zonal wind in the tropical Pacific. *J Atmos Sci* 28(5):702–708
- Madden RA, Julian PR (1972) Description of global-scale circulation cells in the tropics with a 40–50 day period. *J Atmos Sci* 29(6):1109–1123
- Maharana P, Dimri AP (2014a) Impact of initial and boundary conditions on regional winter climate over the Western Himalayas: a fixed domain size experiment. *Global Planet Change* 114:1–13
- Maharana P, Dimri AP (2014b) Study of seasonal climatology and interannual variability over India and its sub-regions using a regional climate model (RegCM3). *J Earth Sys Sci* 123(5):1147–1169
- Misra V, Pantina P, Chan SC, DiNapoli S (2012) A comparative study of the Indian summer monsoon hydroclimate and its variations in three reanalyses. *Clim Dyn* 39:1149–1168
- Mohapatra M, Mohanty UC (2007) Periodicity in intraseasonal variation of summer monsoon rainfall over Orissa, India in relation to synoptic disturbances. *Meteor Atmos Phys* 99:25–42
- Pal J et al (2007) Regional climate modelling for the developing world: the ICTP RegCM3 and RegCNET. *Bull Am Meteor Soc* 88:1395–1409
- Panchawagh NV, Vaidya SS (2011) Link between break/active phases of summer monsoon over India and China. *Curr Sci* 100:1–8
- Raghavan K (1973) Break monsoon over India. *Mon Wea Rev* 101:33–43
- Rajeevan M, Bhatte J (2008) A high resolution daily gridded precipitation dataset (1971–2005) for mesoscale meteorological studies. *Curr Sci* 96:558–562
- Rajeevan M, Bhatte J, Kale JD, Lal B (2006) High resolution daily gridded rainfall data for the Indian region: analysis of break and active monsoon spells. *Curr Sci* 91:296–306
- Rajeevan M, Gadgil S, Bhatte J (2010) Active and break spell of Indian summer monsoon. *J Earth Sys Sci* 119(3):229–247
- Ramamurthy K (1969) Some aspect of the ‘break’ in the Indian southwest monsoon during July and August; Forecasting manual 1–57, No. IV 18, 3, India Met. Dept., Pune, India
- Reynolds RW, Rayner NA, Smith TM, Stokes DC, Wang W (2002) An improved in situ and satellite SST analysis for climate. *J Clim* 15:1609–1625
- Samala BK, Banerjee S, Kaginalkar A, Dalvi M (2013) Study of the Indian summer monsoon using WRF–ROMS regional coupled model simulations. *Atmos Sci Let* 14:20–27
- Seth A, Giorgi F (1998) The effects of domain choice on summer precipitation simulation and sensitivity in a regional climate model. *J Clim* 11(10):2698–2712

- Taraphdar S, Mukhopadhyay P, Goswami BN (2010) Predictability of Indian summer monsoon weather during active and break phases using a high resolution regional model. *Geophys Res Lett* 37:1–6
- Vecchi GA, Harrison DE (2002) Monsoon breaks and subseasonal sea surface temperature variability in the Bay of Bengal. *J Clim* 15:1485–1493
- Zeng X, Zhao M, Dickinson RE (1997) Intercomparison of bulk aerodynamic algorithms for the computation of sea surface fluxes using TOGA COARE and TAO data. *J Clim* 11:2628–2644